

# The pulse train PDA analysis and deinterleaving filter

B. J. Slocumb<sup>a</sup> and E. W. Kamen<sup>b</sup>

<sup>a</sup>Georgia Tech Research Institute

<sup>b</sup>School of Electrical and Computer Engineering  
Georgia Institute of Technology  
Atlanta, GA 30332-0840 USA

## ABSTRACT

This paper develops the pulse train probabilistic data association filter (PT-PDAF) for use in pulse train analysis and deinterleaving applications. The approach is based on a state-space formulation of the pulse train evolution model. The PDA approach overcomes real-world problems of false and missing pulses which cause the basic Kalman filter to break down. Simulations are developed to show that the PT-PDAF approach is superior to a nearest neighbor filter. An augmented PDA approach which incorporates available pulse parameter measurements such as angle of arrival into the PDA algorithm is shown to further improve the filter performance.

**Keywords:** Probabilistic Data Association, Pulse Train, Deinterleaving, Intercept Receiver, Tracking

## 1. INTRODUCTION

A pulse train is a waveform in which a sequence of pulse signals are chained together in a time-ordered fashion, where each pulse is described by a set of feature parameters (e.g., event time, amplitude, carrier frequency, or pulse width). Pulse train processing is performed by a measurement system to accomplish parameter extraction for transmission source characterization or system identification. An important application area of pulse train processing is in electronic defense, specifically the processing of radar pulse measurements by a passive radar intercept receiver.<sup>1</sup> Related problems arise in neurobiological, speech, and medical signal analysis.<sup>2-4</sup> The models and issues associated with the radar intercept application are the focus for this paper.

In practice the passive receiver has little or no *a priori* knowledge about an intercepted pulse train waveform. Individual pulse parameters measured by the receiver may be used for pulse sorting and processing. Inter-pulse parameters are equally important for the processing, and a key parameter is the inter-pulse interval or *pulse repetition interval* (PRI). An estimate of the PRI is derived from the measured pulse time-of-arrival (TOA) values (i.e., a sequence of activation times). The TOA measurements are corrupted by TOA jitter and both false and missing TOA data. Also, the presence of measurements from multiple simultaneous transmission sources complicates the processing. Pulse train analysis is the process of estimating pulse train parameters, and for this work is specifically about PRI estimation. Deinterleaving is the process whereby pulses from a single emitter are sorted from other pulses (both false measurements and interfering sources).

The objective in this paper is to develop the PDA filter for pulse train analysis and deinterleaving. The new work is based on a state-space model which describes the time evolution of the noise-jittered pulse arrival times. A Kalman filter is implemented to estimate and track state parameters of a single pulse train. However, the basic Kalman filter has practical limitations associated with the presence of both false and missing data and multiple interfering sources. We develop the Pulse Train Probabilistic Data Association Filter (PT-PDAF) to significantly improve the robustness to these practical problems. An augmented PT-PDAF is developed which incorporates additional pulse parameters, such as angle of arrival, into the PDA filter. Simulation results are shown for a single pulse train with false and missing measurements. Performance advantages with the PT-PDAF approach are discussed.

---

Other author information: (Send correspondence to B.J.S.) B.J.S.: Email: ben.slocumb@gtri.gatech.edu; Telephone: 404-894-8239; Fax: 404-894-8636; E.W.K.: Email: ed.kamen@ee.gatech.edu; Telephone: 404-894-2994; Fax: 404-894-4641

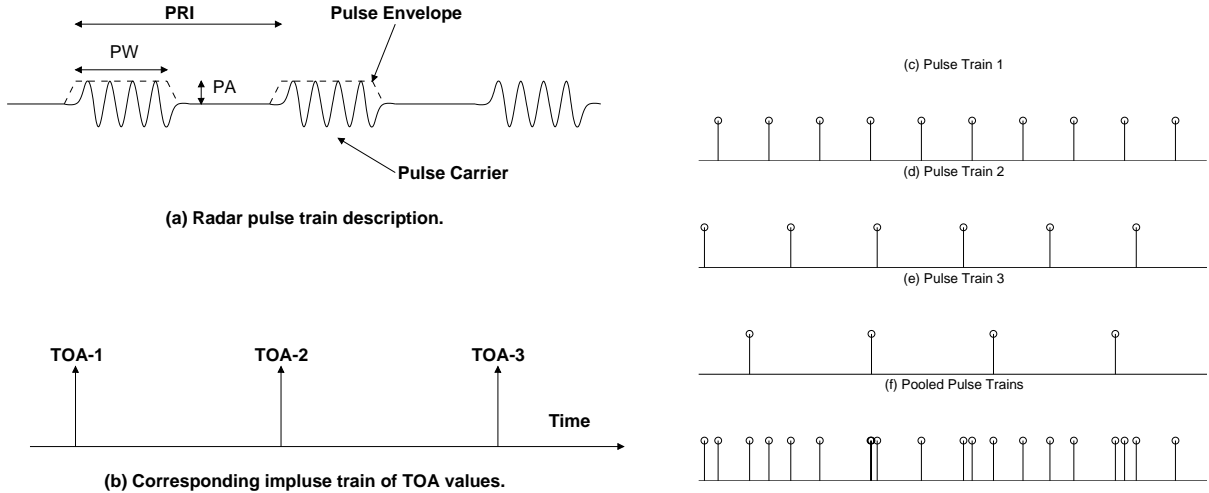


**Figure 1.** Example showing (a) a radar pulse train, and (b) the impulse train for pulse leading-edge TOA values, (c-e) the TOA values from three pulse trains, and (f) the pooled process corresponding to the interleaved TOA values.

## 2. PULSE TRAIN BACKGROUND

Modern radar systems emit pulsed RF energy for the purpose of locating targets in the environment. Passive radar intercept receivers are employed by modern military units to provide information about the active radars in the RF environment. The receivers provide warning and situation awareness (especially from radar-guided missile systems), and perform reconnaissance/surveillance for intelligence data collection. In all cases, the receiver must be able to process and extract pulse train parameters from measurements corrupted by noise and interference.

### 2.1. Measurements

Figure 1-a shows an example radar pulse train with the parameters of interest indicated. The pulses from a single pulse train arrive at the receiver in a time-ordered fashion. The receiver extracts *intra-pulse* parameters from each pulse measurement (TOA, RF frequency, pulse width, amplitude, angle of arrival, and others). The TOA corresponds to the time at which the pulse envelope transcends a threshold value set in the intercept receiver. In many receiver systems, the collected intra-pulse measurements are combined and quantized in a digital data word called the *Pulse Descriptor Word* (PDW). The receiver collects pulse data over a finite observation interval. The receiver *pulse input buffer* consists of the finite collection of PDWs, say  $N$ , measured over the interval,  $\{\text{PDW}(1), \text{PDW}(2), \dots, \text{PDW}(N)\}$ . The input buffer could contain pulse measurements from one or more emitters, and potentially can be corrupted by false and missing measurements.

### 2.2. Pulse train analysis and deinterleaving

Pulse train analysis involves the application of signal processing techniques to quantify the parameters from one emitter pulse train for the purpose of waveform characterization. Typically it is assumed that the pulses from multiple emitters have been presorted except for possibly some false and missing measurements. In this paper, the analysis specifically involves the estimation of the PRI and any PRI variations exhibited over time.

The process of sorting pulses in the pulse input buffer (from multiple sources and false measurements) into individual pulse trains is known as *pulse train deinterleaving*. In this paper, the deinterleaving problem considered is limited to pulse sorting based on the pulse TOA values; other sorting methods based on parameter clustering are available.<sup>5,6</sup> Figure 1 (c-f) describes an example of interleaved TOA data (pooled pulse trains) from three periodic pulse trains. Deinterleaving is conducted by identifying periodic intervals in the pooled TOA data (i.e., extracting the PRIs from the interleaved TOA sequence) to resolve the three constituent pulse trains.

### 2.3. Conventional pulse train analysis and deinterleaving methods

A number of conventional approaches to pulse train analysis and deinterleaving are available. The techniques include: maximum likelihood PRI estimation<sup>7</sup>; PRI estimation via spectrum analysis<sup>8,9</sup>; circular statistics<sup>10</sup> and data folding<sup>11</sup> methods; PRI gating filter<sup>1,12</sup>; sequence search algorithm<sup>1,5</sup>; and the TDOA histogram algorithm.<sup>6,13</sup> Generally, the limitations of these techniques center on robustness or ambiguity problems. Improved robustness is the central goal in the development of the PT-PDAF approach.

## 3. PULSE TRAIN MODELS

Depending on the radar system type, its PRI can be constant or vary in a deterministic or stochastic way. The various emitter types<sup>1</sup> include constant, jittered, staggered, wobulated, sliding, and others. In this paper, we focus on the constant and jittered models. To a certain degree these two types can be used to describe the other models, but limitations exist.

### 3.1. Constant and jittered PRI types

Many radars generate pulses using a *constant* PRI. Peak variations are less than 1% and are incidental (i.e., unintended). The generation time of the  $n$ th pulse from the  $i$ th constant PRI pulse train is

$$t_i(n) = t_i(n - 1) + T_i + w_i(n), \quad (1)$$

where  $T_i$  is the PRI and  $w_i(n)$  is the unintended jitter for the  $n$ th pulse. The first pulse is  $t_i(1) = \phi_i$ , where the unknown phase  $\phi_i$  is taken to be uniformly distributed on  $[0, T_i)$ . No statistical models are discussed in the literature for  $w_i(n)$ , however, as a first approximation we will assume it to be zero-mean white Gaussian with  $\sigma_{w_i} \ll T_i$ .

Some radars intentionally vary the transmission time from pulse to pulse. The variation can be up to 30% of  $T_i$ . Intentional jitter is usually used to defeat some types of jamming techniques. Some jittered waveforms use PRI values selected from a discrete set, while others have the ability to generate pseudo-random values within some range. The model (1) describes the jittered pulse train, but now  $\sigma_{w_i}$  is larger relative to  $T_i$ .

### 3.2. TOA measurements and jitter characterization

Pulse TOA measurements are made at the intercept receiver at times

$$z_i(n) = t_i(n) + \epsilon_i(n), \quad (2)$$

where  $\epsilon_i(n)$  is the *measurement* jitter associated with the  $n$ th pulse TOA measurement. Jitter occurs because of the presence of thermal noise in the receiver and from arrival time quantization. Under high SNR conditions, the RMS value of the jitter due to noise<sup>1</sup> has been evaluated to be

$$\sigma_r = \frac{t_r}{0.8\sqrt{\text{SNR}}}, \quad (3)$$

where  $t_r$  is the rise time of the pulse (between 10% and 90% of the instantaneous pulse amplitude). The rise time will vary from one radar system to the next. Under high SNR conditions, Wiley<sup>1</sup> states that the measurement jitter due to noise is white Gaussian. Additional measurement jitter results from the quantization of the pulse arrival time. The TOA measurement noise  $\epsilon_i(n)$  is the combination of the effects from thermal noise and quantization. The variance of the measurement jitter is

$$\sigma_{\epsilon_i}^2 = \sigma_r^2 + \sigma_q^2. \quad (4)$$

In the pulse train framework, the jitter  $w_i(n)$  is called *cumulative jitter* while  $\epsilon_i(n)$  is termed *noncumulative jitter*. The distinction is important<sup>7</sup> when estimating  $T_i$ .

### 3.3. Conditions that impact pulse train processing

The actual received TOA data stream is rarely equivalent to the idealized model of pooled of impulse trains shown in Figure 1-f. Table 1 lists factors that cause pulses to be either deleted or added from the arrival sequence because of external and receiver system properties. The factors cause non-ideal pulse train sequences to be obtained. Consequently, pulse train analysis and deinterleaving algorithms must be able to handle conditions of *false* and *missing* data in the measured data set.

**Table 1.** Conditions that impact pulse train processing.

Condition	Reason	Comment
Pulse overlap	Pulses from independent sources arrive simultaneously	Only first pulse detected. Pulse parameter measurements corrupted.
Dropped pulses	Misfiring in radar	More typical with magnetrons. Manufacturer specs about 0.25% occurrence rate.
Extraneous pulses	Multipath	Multiple propagation paths resulting from ground and atmosphere reflections.
Intermittent pulse trains	Spatially scanning radar antenna	Only some pulses cross receiver threshold. Pulses measured in bursts.
Pulse Shadowing	Receiver shadow time	Detection circuit phenomenon. No pulses detected for finite time after pulse detection.
False alarms	Noise transcends threshold	False pulse measurement.
Receiver blanking	Turn off receiver momentarily	Required for other systems (transmitters) in use.

#### 4. STATE-SPACE FORMULATION AND KALMAN FILTER

The foundation of the PT-PDAF concepts developed in this paper is a state-space formulation of the TOA measurement process. Koffler<sup>14,15</sup> applied the formulation, but the distinctions of cumulative and noncumulative jitter within the state-space model were identified and analyzed later.<sup>7</sup>

##### 4.1. State-space model

The signal models described in (1) and (2) form the basis for the state-space formulation of the pulse train propagation model developed in.<sup>7,14,15</sup> Define the state vector to be

$$\mathbf{x}_i(n) = \begin{bmatrix} T_i(n) \\ t_i(n) \end{bmatrix}. \quad (5)$$

Here, the static parameter  $T_i$  has been incorporated into the state vector with the parameter  $t_i(n)$  which varies with the pulse number  $n$ . In the vector  $T_i$  becomes  $T_i(n)$  even though the PRI is not a function of the pulse number. The purpose for doing this is to estimate the static parameter through a state estimation procedure.

Using the defined state vector, the *state equation* which describes the evolution of the pulse train is

$$\mathbf{x}_i(n+1) = \mathbf{F}_i \mathbf{x}_i(n) + \mathbf{w}_i(n), \quad (6)$$

and the *measurement equation* is

$$z_i(n) = \mathbf{H}_i \mathbf{x}_i(n) + \epsilon_i(n). \quad (7)$$

The matrices for the state and measurement equations are defined as

$$\mathbf{F}_i = \begin{bmatrix} 1 & 0 \\ 1 & 1 \end{bmatrix}, \quad \mathbf{H}_i = [ 0 \quad 1 ]. \quad (8)$$

Note that it becomes necessary to create a process noise vector  $\mathbf{w}_i(n)$  with a zero component associated with  $T_i(n)$ ,

$$\mathbf{w}_i(n) = \begin{bmatrix} 0 \\ w_i(n) \end{bmatrix}, \quad (9)$$

where the noise vector is taken to be white Gaussian,  $\mathbf{w}_i(n) \sim \mathcal{N}(0, \mathbf{Q}_i)$ , with

$$E\{\mathbf{w}_i(j)\mathbf{w}_i'(k)\} = \delta_{jk} \mathbf{Q}_i, \quad \mathbf{Q}_i = \begin{bmatrix} 0 & 0 \\ 0 & \sigma_{w_i}^2 \end{bmatrix}. \quad (10)$$

In some emitters,  $T_i$  may drift over time in which case it becomes useful to include a noise component for  $T_i(n)$  by setting  $\mathbf{Q}_i(1,1) = \sigma_{T_i}^2 > 0$ .

In the formulation the measurement jitter is taken to be white Gaussian,  $\epsilon_i(n) \sim \mathcal{N}(0, R_i)$ , with  $E\{\epsilon_i(j)\epsilon_i(k)\} = \delta_{jk} R_i$ , and where  $R_i = \sigma_{\epsilon_i}^2$  is a scalar.

## 4.2. Kalman filter implementation

Using the state-space formulation in (6) and (7), a Kalman filter can be implemented to track and process the measurements. The Kalman filter state estimate at pulse index  $k$  is

$$\hat{\mathbf{x}}_i(k|k) = \begin{bmatrix} \hat{T}_i(k|k) \\ \hat{t}_i(k|k) \end{bmatrix}. \quad (11)$$

The value of  $\hat{T}_i(k|k)$  provides a “smoothed” estimate of  $T_i$  using the measurements up to pulse number  $k$ , while the estimate  $\hat{t}_i(k|k)$  “tracks” the pulse TOA sequence through the pulse input buffer. The standard discrete-time implementation of the Kalman filter<sup>16</sup> follows:

1. Initialize the state estimate  $\hat{\mathbf{x}}_i(2|2)$  and covariance  $\mathbf{P}_i(2|2)$ . Initialization is accomplished using the two-point differencing method<sup>16</sup> which guarantees *Finite Sample Consistency* such that the mean and covariance of the state estimate match the true values.

2. Kalman Gain Update Equation:

$$\mathbf{L}_i(k) = \mathbf{P}_i(k|k-1)\mathbf{H}_i' S_i^{-1}(k), \quad (12)$$

$$\mathbf{P}_i(k|k-1) = \mathbf{F}_i \mathbf{P}_i(k-1|k-1) \mathbf{F}_i' + \mathbf{Q}_i, \quad S_i(k) = \mathbf{H}_i \mathbf{P}_i(k|k-1) \mathbf{H}_i' + R_i. \quad (13)$$

3. State Estimate Update Equation:

$$\hat{\mathbf{x}}_i(k|k) = \mathbf{F}_i \hat{\mathbf{x}}_i(k-1|k-1) + \mathbf{L}_i(k) (z_i(k) - \mathbf{H}_i \mathbf{F}_i \hat{\mathbf{x}}_i(k-1|k-1)). \quad (14)$$

4. State Covariance Update Equation:

$$\mathbf{P}_i(k|k) = (\mathbf{I}_2 - \mathbf{L}_i(k)\mathbf{H}_i) \mathbf{P}_i(k|k-1). \quad (15)$$

5. Iterate the filter using steps 2–4 for  $k = 2, \dots, N_i$ .

## 4.3. Kalman filter implementation issues

When the Kalman filter is implemented using the basic formulation, several important implementation issues arise which limit the viability of the approach:

- The covariance parameters ( $\mathbf{Q}_i, R_i$ ) are unknown in the pulse train model. Approximate values or adaptive methods are required to overcome this limitation. Model mismatch can cause performance degradation.<sup>17</sup>
- The presence of false and missing data or the presence of multiple pulse trains causes anomalies in the state model and leads to degraded filter performance. Data association concepts are needed to overcome this limitation.
- A discrete-time state-space model and Kalman filter are used for pulse train tracking and analysis. However, in the model the discrete index  $k$  is the *pulse number* and not the *sample time*. This property introduces unique problems because the entire state-space model breaks down when anomalies in the data measurement sequence occur.

REMARK 1. *The uniqueness of the pulse train discrete-time model is critical for understanding the requirements for the data association approaches. Specifically, the combination of measurements  $\{z_i(n)\}$  and  $\{z_j(n)\}$  from two sources, for example, does not lead to the usual data association model where two measurements are available at each sample index. Instead, the measurements are intermixed into one event stream, and the origin of each event is ambiguous (see Figure 1).*

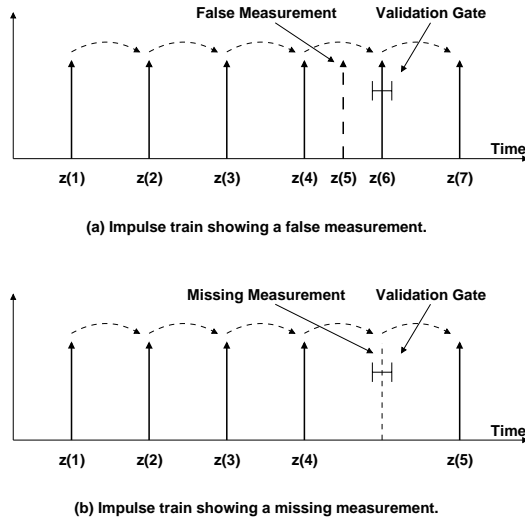


**Figure 2.** Measurement validation: (a) the gate allows a false measurement to be skipped, and (b) a missing pulse to be detected.

#### 4.4. Nearest neighbor standard filter (NNSF)

Koffler<sup>14,15</sup> applied the NNSF to the pulse train deinterleaving problem. Simulation results showed that the adaptive gate size provided by the Kalman filter measurement validation technique, compared to a fixed gate size, improved the deinterleaving performance. While this work demonstrated the utility of the Kalman filter approach, issues associated with false/missing data were not addressed and the application of the NNSF was only used to handle simultaneous emitters. Also, aspects associated with PRI estimation and the estimation accuracy were not discussed. In this paper, we will use the NNSF as a benchmark to which we can compare the PT-PDAF.

### 5. THE PULSE TRAIN PDA FILTER

To remedy the shortcomings of the basic Kalman filter approach, extensions are needed which make the approach robust to inherent problems in the operational environment. Here, we formulate a new Pulse Train Probabilistic Data Filter (PT-PDAF) approach. This technique is designed to accommodate the false and missing data problems.

*REMARK 2. The general PDA Filter approach cannot be directly applied to the pulse train problem. This work develops the necessary modification of the framework to handle the unique nature of the TOA event sequence. Specifically, a discrete-time model is used for the pulse index numbers, but only a single measurement is available at each index. Association must be accomplished over measurements in a local time interval instead.*

#### 5.1. Measurement validation

Before we can develop the PT-PDAF, we must define the measurement validation procedure. Within the algorithm, measurement validation *selects* a specific collection of TOA measurements (from the total available) to be processed by the state estimator. The concept is to define a “gate region” that corresponds to a time segment in which the next pulse TOA is expected to occur. This overcomes two problems. When false TOA measurements are present the filter can “skip over” any false TOAs in the measurement sequence, and find the next “appropriate” TOA value to include in the filter. This is shown in Figure 2-a. When missing TOA measurements occur, the presence of no TOA measurements in the gate indicates a missing TOA. The filter can then “coast ahead” to the next expected measurement,  $\hat{z}_i(k + 2|k)$ , and continue processing without violating the state-space model. This is shown in Figure 2-b.

The validated measurements are identified as follows. Suppose that  $\{z(n)\}_{n=1}^N$  constitutes all TOA measurements, while  $\{z_i(k)\}_{k=1}^{N_i}$  are only those associated with the  $i$ th pulse train, where  $N_i \leq N$  and  $\{z_i(k)\} \subseteq \{z(n)\}$ . Suppose

the Kalman filter has processed data up to pulse number  $k$ , with  $\hat{\mathbf{x}}_i(k|k)$  available. The predicted TOA measurement for pulse number  $k + 1$  is  $\hat{z}_i(k + 1|k) = \mathbf{H}_i \mathbf{F}_i \hat{\mathbf{x}}_i(k|k)$ . The next measurement from the  $i$ th pulse train,  $z_i(k + 1)$ , is now assumed to be normally distributed about this predicted TOA value,

$$z_i(k + 1|k) \sim \mathcal{N}(\hat{z}_i(k + 1|k), S_i(k + 1)), \quad (16)$$

where  $S_i(k + 1)$  is the measurement covariance. From the set of all available of TOA measurements,  $\{z(1), \dots, z(N)\}$ , the set of validated measurements is formed as

$$\begin{aligned} \mathcal{Z}_i(k + 1, \gamma) &= \{z(\ell) : (z(\ell) - \hat{z}_i(k + 1|k))' S_i(k + 1)^{-1} (z(\ell) - \hat{z}_i(k + 1|k)) \leq \gamma\} \\ &= \{z_{i,1}(k + 1), z_{i,2}(k + 1), \dots, z_{i,m(k+1)}(k + 1)\}. \end{aligned} \quad (17)$$

In this expression,  $\ell \in \{1, 2, \dots, N\}$  is the index over all the measured TOAs, and  $\gamma$  is the gate threshold parameter. The set  $\{z_{i,j}(k)\}$  defines a sub-collection of TOA measurements  $\{z(n + 1), \dots, z(n + m_i(k))\} \subset \{z(\ell)\}$ . This notation identifies the  $j$ th validated measurement,  $j \in \{1, 2, \dots, m(k)\}$ , corresponding to the  $k$ th pulse,  $k \in \{1, 2, \dots, N_i\}$ , of the  $i$ th pulse train. The value  $m(k + 1)$  is the number of available measurements in the gate at index  $k + 1$ .

The Normalized Innovation Squared (NIS) is formed as

$$\varepsilon_{i,j}(k + 1) = (z_{i,j}(k + 1) - \hat{z}_i(k + 1|k))' S_i(k + 1)^{-1} (z_{i,j}(k + 1) - \hat{z}_i(k + 1|k)), \quad (18)$$

which under the Gaussian assumption (16) has a Chi-square distribution with one degree of freedom. The threshold  $\gamma$  is selected from the Chi-square distribution table so that the probability the next pulse is within the gate,  $P_G = \Pr\{z_i(k + 1) \in \mathcal{Z}_i(k + 1, \gamma)\}$ , achieves a desired value.

**REMARK 3.** *The extraction of the subset of TOA measurements  $\{z_{i,j}(k)\}$  from  $\{z(\ell)\}$  is the key concept in the modification of the general PDA approach to the pulse train processing application. It generates the measurement set on which data association is performed.*

## 5.2. The pulse train PDA filter algorithm

Suppose that the PT-PDAF has been initialized and processed up to pulse index  $k$  and that the usual PDA filter assumptions<sup>18</sup> hold. Then the implementation of the PT-PDAF algorithm can be summarized as follows:

1. Measurement Validation: the available measurements are identified as those within the validation gate,

$$\begin{aligned} \mathcal{Z}_i(k + 1, \gamma) &= \{z(\ell) : (z(\ell) - \hat{z}_i(k + 1|k))' S_i(k + 1)^{-1} (z(\ell) - \hat{z}_i(k + 1|k)) \leq \gamma\} \\ &= \{z_{i,1}(k + 1), z_{i,2}(k + 1), \dots, z_{i,m(k+1)}(k + 1)\}. \end{aligned} \quad (19)$$

2. State Estimate Update: the estimate is computed from the weighted sum of the state estimates formed using the validated measurements,

$$\hat{\mathbf{x}}_i(k|k) = \sum_{j=0}^{m(k)} \beta_j(k) \hat{\mathbf{x}}_{i,j}(k|k), \quad (20)$$

where  $\hat{\mathbf{x}}_{i,j}(k|k)$  is the updated state conditioned on the  $j$ th pulse TOA in the validated TOA set,

$$\hat{\mathbf{x}}_{i,j}(k|k) = \hat{\mathbf{x}}_i(k|k - 1) + \mathbf{L}_i(k) \nu_{i,j}(k). \quad (21)$$

The innovation associated with the  $j$ th validated TOA is

$$\nu_{i,j}(k) = z_{i,j}(k) - \hat{z}_i(k|k - 1). \quad (22)$$

In the PT-PDAF implementation, the Kalman gain is computed in the usual way,

$$\mathbf{L}_i(k) = \mathbf{P}_i(k|k - 1) \mathbf{H}_i' S_i(k)^{-1}. \quad (23)$$

The *association probabilities*  $\{\beta_j(k); j = 0, 1, \dots, m(k)\}$  are computed for all the validated measurements at sample number  $k$ . This probability represents the likelihood that  $z_{i,j}(k)$  is the correct measurement for the  $i$ th pulse train. Bar-Shalom and Li<sup>18</sup> give the calculation of the probabilities,

$$\beta_j(k) = \begin{cases} \frac{e_j}{b + \sum_{r=1}^{m(k)} e_r} & j = 1, 2, \dots, m(k), \\ \frac{b}{b + \sum_{r=1}^{m(k)} e_r} & j = 0, \end{cases} \quad (24)$$

where

$$e_j = \exp\left(-\frac{1}{2}\nu_{i,j}(k)'S_i(k)^{-1}\nu_{i,j}(k)\right), \quad (25)$$

$$b = \left(\frac{2\pi}{\gamma}\right)^{1/2} \cdot \frac{m(k)}{2} \cdot \frac{1 - P_D P_G}{P_D}. \quad (26)$$

3. Covariance Update: the covariance update incorporates uncertainty in the measurement origin,

$$\mathbf{P}_i(k|k) = \beta_0(k)\mathbf{P}_i(k|k-1) + (1 - \beta_0(k))\mathbf{P}_i^c(k|k) + \tilde{\mathbf{P}}_i(k), \quad (27)$$

In this expression, there are three components to the covariance update calculation. The first term on the right-hand side,  $\beta_0(k)\mathbf{P}_i(k|k-1)$ , accounts for the possibility that the true measurement is not in the gate. The second term,  $(1 - \beta_0(k))\mathbf{P}_i^c(k|k)$ , is the weighted covariance for the correct measurement,

$$\mathbf{P}_i^c(k|k) = \mathbf{P}_i(k|k-1) - \mathbf{L}_i(k)S_i(k)\mathbf{L}_i(k)'. \quad (28)$$

The third term is called the ‘‘spread of the innovations term,’’

$$\tilde{\mathbf{P}}_i(k) = \mathbf{L}_i(k) \left( \sum_{j=1}^{m(k)} \beta_j(k)\nu_{i,j}(k)\nu_{i,j}(k)' - \nu_i(k)\nu_i(k)' \right) \mathbf{L}_i(k)'. \quad (29)$$

This term increases the covariance, and it comes about because of the effect of the measurement origin uncertainty in the filter implementation.

4. Filter and Covariance Prediction (identical to the basic Kalman filter):

$$\hat{\mathbf{x}}_i(k+1|k) = \mathbf{F}_i\hat{\mathbf{x}}_i(k|k), \quad (30)$$

$$\mathbf{P}_i(k+1|k) = \mathbf{F}_i\mathbf{P}_i(k|k)\mathbf{F}_i' + \mathbf{Q}_i, \quad (31)$$

$$\hat{z}_i(k+1|k) = \mathbf{H}_i\hat{\mathbf{x}}_i(k+1|k), \quad (32)$$

$$S_i(k+1) = \mathbf{H}_i\mathbf{P}_i(k+1|k)\mathbf{H}_i' + R_i. \quad (33)$$

PT-PDAF track initialization in the presence of false and missing data is an important problem. A form of the Sequence Search Algorithm was implemented for initialization, and limited success was achieved. For the ongoing work, exact initialization was assumed. Other track filter initialization algorithms specific to multiple target tracking (MTT) applications are available,<sup>18</sup> and ongoing work is developing these techniques.

## 6. AUGMENTED PULSE TRAIN PDA FILTERS

In many pulse train processing applications, pulse measurement parameters such as angle-of-arrival (AOA) or RF frequency are available in addition to the TOA. Two possible approaches exist as to how this available ‘‘information’’ can be utilized within the PT-PDAF framework. One approach<sup>18</sup> is to use the parameters in the calculation of the PDA weights. A second approach<sup>19</sup> is to incorporate the parameters into the state vector.

### 6.1. Augmented PDA with feature parameters

Bar-Shalom and Li<sup>18</sup> have developed a method to extend the PDAF when measurements of a *target feature* are available called the *Augmented PDA with Feature Measurements* approach. The additional feature measurements can be used to discriminate “target” measurements from “clutter” using a statistical weighting in the PDA framework. A fundamental property is that density functions for the feature parameters must be known (or assumed) for both the target and clutter false measurements. Suppose  $\theta(k)$  is a feature parameter (e.g., angle of arrival) corresponding to TOA measurement  $z(k)$ . Let  $\theta(k)$  have the density function  $p_T(\theta(k))$  if the measurement is associated with a pulse train (target), and density  $p_C(\theta(k))$  if the measurement is attributed to noise (clutter). Define the target-to-clutter feature likelihood ratio as

$$L_{T/C}(\theta(k)) = \frac{p_T(\theta(k))}{p_C(\theta(k))}. \quad (34)$$

Then the association probabilities in (25) are augmented<sup>18</sup> as follows,

$$e_j = \exp\left(-\frac{1}{2}\nu_{i,j}(k)'S_i(k)^{-1}\nu_{i,j}(k)\right) \cdot L_{T/C}(\theta(k)). \quad (35)$$

For the pulse train problem, a reasonable assumption is that parameter measurements have a Gaussian distribution,  $p_T(\theta_i(k)) = \mathcal{N}(\bar{\theta}, \sigma_\theta^2)$ , while the noise (clutter) can be assumed to have a uniform distribution,  $p_C(\theta_i(k)) = \mathcal{U}(\theta_{min}, \theta_{max})$ . Note that this implementation of the augmented PDA approach requires knowledge of four parameters,  $\{\bar{\theta}_i, \sigma_{\theta_i}, \theta_{min}, \theta_{max}\}$ . Typically, the mean parameter value,  $\bar{\theta}_i$ , could not reasonably be assumed available (e.g., the true angle of arrival), but one might use an estimate from a previous receiver dwell.

### 6.2. Augmented state pulse train PDA filter

The second approach for using parameter measurements within the PT-PDAF is to include them in an *augmented state vector*,  $\mathbf{x}_i(n) = [\theta_i(n) \ T_i(n) \ t_i(n)]'$ . As explained in Ref. 19, the implementation requires new augmented definitions for the matrices  $\mathbf{F}_i$ , and  $\mathbf{H}_i$ , and the measurement vector,  $\mathbf{z}_i(n) = [\theta_i(n) \ t_i(n)]'$ . The dimension of  $\mathbf{Q}_i$  is extended, but we set  $\mathbf{Q}_i(1, 1) = 0$ . A new measurement noise covariance matrix  $\mathbf{R}_i$  is defined which has the diagonal elements  $\sigma_{\theta_i}^2$  and  $\sigma_{t_i}^2$ . Then the PT-PDAF is implemented using the augmented model.

Through the decoupling<sup>19</sup> of terms in the Normalized Innovation Squared,  $\nu_i(k)'S_i^{-1}(k)\nu_i(k)$ , the computation of  $e_j$  in (24) for the augmented state vector becomes

$$e_j = \exp\left(-\frac{1}{2}\nu_{i,j}(k)'S_i^{-1}(k)\nu_{i,j}(k)\right) \cdot e_{\theta_j}, \quad (36)$$

where

$$e_{\theta_j} = \exp\left(-\frac{1}{2}\nu_\theta(k)'S_\theta^{-1}(k)\nu_\theta(k)\right). \quad (37)$$

The first part of (36) is equivalent to (25),  $\nu_\theta(k)$  is the innovation associated with  $\theta(k)$ , and  $S_\theta(k)$  is the portion of the measurement covariance which corresponds to  $\nu_\theta(k)$ . This shows that the Normalized Innovation Squared for  $\theta_i(k)$  provides another weighting component within the PDA algorithm. If the innovation  $\nu_\theta(k)$  is big, then it causes  $e_j$  and the association weight  $\beta_j$  to become small. Notice that the only parameter that is required to be known with in the Augmented State approach is  $R_\theta = \sigma_\theta^2$ .

### 6.3. Comparison of Approaches

A comparison of the association weights (37) and (35) shows that that the likelihood ratio weight applied in the Augmented PDA with Feature Measurements is very similar to the weight applied in the Augmented State PT-PDAF. Both use a normalized squared error measure in the exponential weight. With the Augmented State approach the normalized innovation squared error is used, whereas the Feature Measurements approach measures the error from the true parameter value  $\bar{\theta}$ . The normalization factor in the augmented state approach is  $S_\theta(k)$ , and it is shown<sup>19</sup> that  $S_\theta(k) \rightarrow R_\theta \equiv \sigma_\theta^2$ . Therefore, when  $\hat{\theta}_i(k) \rightarrow \bar{\theta}$ , the association weights in the two approaches converge. We conclude that by evaluating the analytical expressions for the two approaches, the weights are very similar in form. The advantage of the Augmented State PT-PDAF approach is 1) that the parameters are used in the data validation procedure which helps to eliminate more of the clutter measurements, and 2) the mean parameter value  $\bar{\theta}$  does not have to be known *a priori*.

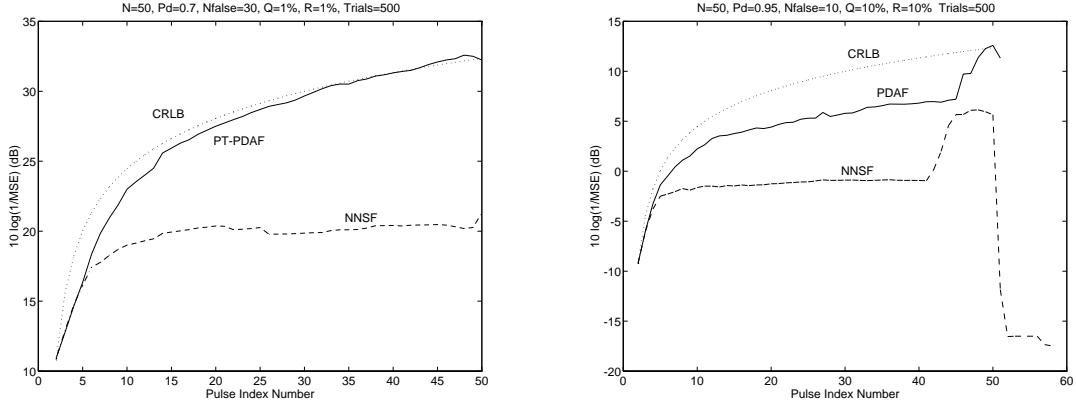


**Figure 3.** MSE performance for the NNSF and PT-PDAF PRI estimate versus the pulse number for the cases of (a) 1% NCJ and CJ, and 30% missing and 60% false measurements, and (b) 10% NCJ and CJ, and 5% missing and 20% false measurements.

## 7. SIMULATION RESULTS

Monte Carlo simulations were developed to assess the mean-squared error (MSE) performance of the PT-PDAF approach. The results described here pertain to the case of a single pulse train corrupted by both false and missing measurements. The simulation results show a comparison between the PT-PDAF MSE performance and the NNSF MSE performance. Results are also shown for the two augmented techniques described for incorporating other pulse parameter measurements into the PT-PDAF.

### 7.1. The Pulse Train PDA Filter versus the NNSF

Figure 3-a shows plots of the PRI MSE performance for the NNSF, PT-PDAF, and the CRLB.<sup>7</sup> In this plot the noncumulative jitter  $\epsilon_i(k)$  (NCJ) and cumulative jitter  $w_i(k)$  (CJ) were set so  $3\sigma/T_i = 0.01$  (i.e., 1% jitter), while 30% of the TOAs were removed and 30 uniformly distributed random false TOAs were added. The performance parameter calculated in the plot is  $10 \log(1/\text{MSE})$  for the PRI estimate versus the pulse index number. As can be seen, the PDAF performance achieves the CRLB and is superior to that of the NNSF. In the example, the CRLB corresponds to the bound for optimal performance of an estimator using perfect data (i.e., no false or missing data). Figure 3-b shows the case where the jitter level is more substantial (the NCJ and CJ are 10%), and where there is 5% missing and 20% false measurements. This example shows that higher jitter level causes the PT-PDAF performance to degrade from the CRLB, but that the performance is still better than that of the NNSF.

In the development of the simulations, the following general observations about performance were made:

- At low levels of false and missing data (e.g., 1%), both the PT-PDAF and the NNSF techniques perform well. Simulations showed that the MSE performance approximates the CRLB.
- The jitter variance levels influence the performance outcome because, for higher jitter levels, the predicted position of the next TOA is more uncertain. Hence, the validation gate must be expanded which makes the susceptibility to false measurements greater.
- The NNSF appears to be much more sensitive to missing data than the PT-PDAF.
- On occasion, either (or both) of the filters will “lose track” and diverge to an incorrect value. The divergent estimate leads to a large error, and it causes the MSE estimate (formed in the Monte Carlo trials) to differ significantly from the CRLB.
- Since the number of false and missing TOAs in each data set is unknown to the filter, the pulse count (the  $x$ -axis) can be different for each trial. Hence, the number of trials averaged for each index is different.

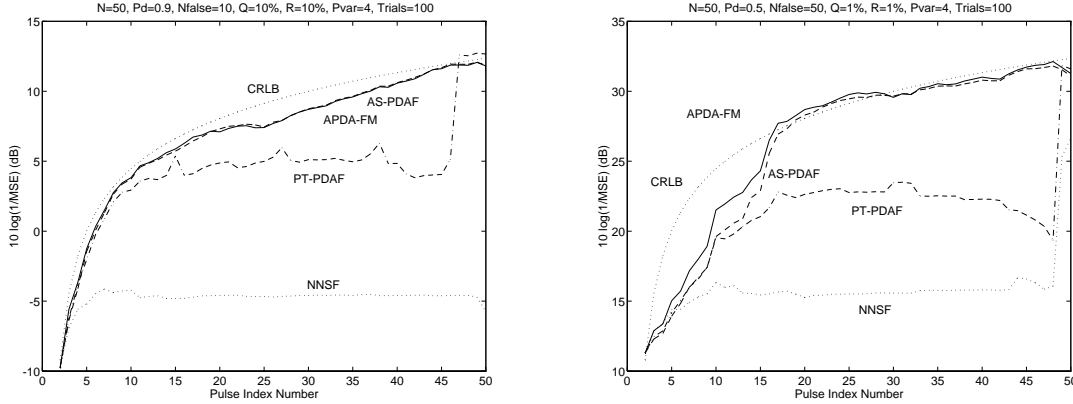


**Figure 4.** MSE performance of the PRI estimate for the Augmented State PT-PDAF (labeled AS-PDAF) and Augmented PDA with Feature Measurements (labeled APDA-FM) methods for the cases of (a) 10% missing data and 10% false data, and (b) 50% missing data and 100% false data.

- The jumps in the MSE plots at about index 40 occur because some number of “bad trial” tracks (i.e., divergent estimates) terminated there. All of the “good trials” continued out to pulse index 50 (the actual number of pulses in the original pulse train). One or two trials continued processing past index 50 because of coasting; these estimates should be considered as outliers.

In summary, the PT-PDAF provides accurate state estimates under moderate levels of false/missing data. The performance depends on the TOA jitter level. On occasion, the filter will diverge to the wrong value and this leads to a “suboptimal performance” MSE characterization. The NNSF provides good estimates most of the time in light false/missing data conditions. However, the NNSF diverges more frequently than the PT-PDAF, thus it has a poorer MSE performance characterization.

## 7.2. Augmented PT-PDAF simulations

To demonstrate the augmented PT-PDAF techniques described in Section 6, a single additional parameter (the angle of arrival) was assumed available with each pulse TOA measurement. The pulse train AOA measurements were assumed to have a variance of  $\sigma_{\theta}^2 = 4$  and a mean of  $\bar{\theta} = 45$ . Both were assumed known. The false measurements were given random AOA values spread over the interval  $[0, 90]$ .

Figure 4-a shows the simulation results for the case of 10% noncumulative and cumulative jitter, and 10% missing data and 20% false measurements. As expected, the Augmented PDA with Feature Measurements (labeled APDA-FM) and Augmented State PT-PDAF (AS-PDAF) approaches show better MSE performance than the PT-PDAF because the additional parameter information enhances the false measurement discrimination. The NNSF is worse than all the PT-PDAF methods. Figure 4-a also shows that the two augmented PT-PDAF methods have (near) identical performance. This is expected since the weights created by the two methods converge to the same value. Figure 4-b shows results for the case where there is heavy measurement corruption (50% missing data and 100% false measurements). In this example the jitter is low (1% noncumulative and cumulative jitter). The plot shows that the additional parameter information significantly enhances the false measurement discrimination—which is the primary benefit of the approach.

In summary, the two techniques for incorporating pulse parameter measurement information (such as angle of arrival) into the PT-PDAF improve the estimation performance. The two approaches provide near identical performance, while the Augmented State PT-PDAF requires less knowledge about the parameter statistical properties.

## 8. CONCLUSIONS

In this paper, we developed the pulse train PDA filter approach for pulse train processing applications. The technique is based on a state-space formulation of the pulse train evolution model. The use of data association techniques is

required to handle the real-word problem associated with false and missing TOA data. Simulations showed that the PT-PDAF approach is superior to the NNSF approach. Also, an augmented PT-PDAF approach was developed which showed how additional pulse parameter measurements could be used within the PDA framework to improve the filter performance. The work in this paper specifically focused on the processing of a data from a single pulse train which is corrupted by false and missing data. Using some of the data structures in Ref. 20, work is in progress to extend the PDA approach to the case of multiple simultaneous pulse trains (the full *deinterleaving* problem).

## REFERENCES

1. R. G. Wiley, *Electronic Intelligence: The Analysis of Radar Signals*, Artech House, Norwood, MA, 2nd ed., 1982.
2. M. Abeles and M. H. Goldstein, "Multispikes train analysis," *Proceedings of the IEEE* **65**, pp. 763–773, May 1977.
3. E. Yair and I. Gath, "On the use of pitch power spectrum in the evaluation of vocal tremor," *Proceedings of the IEEE* **76**, pp. 1166–1175, September 1988.
4. Y. T. Zhang, C. B. Frank, R. M. Rangayyan, and G. D. Bell, "Mathematical modeling and spectrum analysis of the physiological patello-femoral pulse train produced by slow knee movements," *IEEE Transactions on Biomedical Engineering* **39**, pp. 971–979, September 1992.
5. C. L. Davies and P. Hollands, "Automatic processing for ESM," *IEE Proceedings, F (Radar and Signal Processing)* **129**, pp. 164–171, June 1982.
6. J. A. V. Rogers, "ESM processor system for high pulse density radar environments," *IEE Proceedings, F (Radar and Signal Processing)* **132**, pp. 621–625, December 1985.
7. D. A. Gray, B. J. Slocumb, and S. D. Elton, "Parameter estimation for periodic discrete event processes," *Proceedings of IEEE ICASSP* **4**, pp. 93–96, 1994.
8. M. S. Bartlett, "The spectral analysis of point processes," *Journal of the Royal Statistical Society, B* **25**, pp. 264–296, 1963.
9. E. Fogel and M. Gavish, "Parameter estimation of quasi-periodic sequences," *Proceedings of IEEE ICASSP* **4**, pp. 2348–2351, 1988.
10. S. D. Elton and D. A. Gray, "The application of circular statistics to specific radar pulse train detection," *Proceedings of EUSIPCO* **1**, pp. 284–287, 1994.
11. J. Perkins and I. Coat, "Pulse train deinterleaving via the hough transform," *Proceedings of IEEE ICASSP* **3**, pp. 197–200, 1994.
12. B. J. Brown, "Pulse repetition frequency discriminator with complete harmonic suppression," *IEEE Transactions on Aerospace and Electronic Systems* **9**, pp. 112–113, January 1973.
13. H. K. Mardia, "New techniques for the deinterleaving of repetitive sequences," *IEE Proceedings, F (Radar and Signal Processing)* **136**, pp. 149–154, August 1989.
14. E. T. Kofler, "A new approach to the pulse train deinterleaving problem," Master's thesis, University of California, Los Angeles, 1987.
15. E. T. Kofler and C. T. Leondes, "New approach to the pulse train de-interleaving problem," *International Journal on Systems Science* **20**(12), pp. 2663–2671, 1989.
16. Y. Bar-Shalom and X. R. Li, *Estimation and Tracking: Principles, Techniques, and Software*, Artech House, Norwood, MA, 1993.
17. S. D. Elton and B. J. Slocumb, "Robust Kalman filter for estimation and tracking of a class of periodic discrete event processes," *Fourth International Symposium on Signal Processing and Its Applications* **1**, pp. 262–265, August 1996.
18. Y. Bar-Shalom and X. R. Li, *Multitarget-Multisensor Tracking: Principles and Techniques*, YBS, Storrs, CT, 1995.
19. B. J. Slocumb, "A comparison of two augmented PDA filters," *Proceedings of the American Control Conference*, June 1997.
20. J. B. Moore and V. Krishnamurthy, "De-interleaving pulse trains using discrete-time stochastic dynamic-linear models," *IEEE Transactions on Signal Processing* **42**, pp. 3092–3103, November 1994.